J Neurophysiol 100: 1265–1277, 2008.
First published July 16, 2008; doi:10.1152/jn.00048.2008.

A Novel Type of Auditory Responses: Temporal Dynamics of 40-Hz Steady-State Responses Induced by Changes in Sound Localization

Bernhard Ross
Rotman Research Institute, Baycrest Centre, University of Toronto, Toronto, Ontario, Canada

Submitted 13 January 2008; accepted in final form 14 July 2008

Ross B. A novel type of auditory responses: temporal dynamics of 40-Hz steady-state responses induced by changes in sound localization. *J Neurophysiol* 100: 1265–1277, 2008. First published July 16, 2008; doi:10.1152/jn.00048.2008. Magnetoencephalographic responses to 40-Hz amplitude-modulated tones of 4-s duration were recorded in young, middle-aged, and older healthy participants. Interaural phase difference (IPD) in the sound carrier was changed during stimulus presentation from 0 to 180°, resulting in perceptual change from focal to spacious sound. The stimulus modulation elicited synchronized gamma-band oscillations, the 40-Hz auditory steady-state response (ASSR). Equivalent current dipoles were localized in primary auditory cortices. Waveforms of cortical activity showed a decrement in ASSR amplitude 100 ms after stimulus IPD change and modification of ASSR phase, which was maximally 90°, corresponding to 6-ms delay. Time courses of ASSR phase deviation constituted a novel auditory response. The amount of ASSR phase change decreased with increasing stimulus frequency and revealed upper limits for physiological IPD detection. Thresholds for IPD detection were found close to 1,500 Hz in the young, around 1,250 Hz in the middle-aged group, and around 1,000 Hz in the older group. Whereas the ASSR change response revealed aging-related decline of binaural hearing, the amplitude of 40-Hz response and the size of the ASSR change response were not affected by aging. Additional ASSR change responses were recorded at a high rate of stimulus changes every 400 ms. ASSR response detection at this rate was superior to response detection based on the auditory-evoked P1–N1–P2 response. Responses to changes from focal to spacious sound were larger than those in the reverse direction. The ASSRs were interpreted in relation to oscillatory gamma-band activity representing auditory object representation.

INTRODUCTION

Binaural hearing enhances the signal-to-noise ratio in a multispeaker environment because the ability to localize sound in space helps to separate relevant speech from competing noise (Culling et al. 2004; Hawley et al. 2004). Deficits in binaural hearing may decrease the ability of elderly subjects to understand speech in noisy environments or with multiple simultaneous speakers. Recently, we recorded auditory-evoked responses to changes in the interaural phase difference (IPD) of pure tones to study how aging affects binaural hearing (Ross et al. 2007a). The stimuli were amplitude-modulated (AM) tones of 4-s duration. During the first 2 s the same sounds were presented to both ears (diotic stimulation) and for the second half the sounds in both ears were of opposite polarity (dichotic stimulation). The IPD change from 0 to 180° was perceived as sound originating from a single source in the center of the head, switching to sound that was diffusely localized around the head. The IPD change elicited an initial positive–sharp negative–slow positive (P1–N1–P2) wave similar to the sound onset response in the magnetoencephalographic (MEG) recorded auditory-evoked responses (AEFs). According to the duplex theory of binaural hearing only frequencies $\lesssim$1,500 Hz contribute to binaural hearing based on IPD (Stevens 1936). A corresponding physiological threshold close to 1,250 Hz was found in recording of AEF to IPD changes at various carrier frequencies in young subjects (Ross et al. 2007b). Physiological and behavioral thresholds for IPD change detection were lower in older subjects and the effect was already significant in the middle-aged group (Ross et al. 2007a).

To keep sudden changes in the stimulus phase from being perceived as a click-like sensation, we used an AM stimulus and changed the phase at the minimum amplitude (Fig. 1). Although the AM was otherwise irrelevant to IPD change detection, the modulation frequency of 40 Hz was chosen to evoke auditory steady-state responses (ASSRs) of maximal amplitude (Galambos et al. 1981; Picton et al. 2003; Purcell et al. 2004; Rees et al. 1986; Ross et al. 2000). In previous studies we found that the ASSR was strongly modulated by changes in the periodicity of the AM sound stimulus (Ross and Pantev 2004) or in the presence of an interfering stimulus (Ross et al. 2005b). The hypothesis for the current study was that IPD changes—i.e., sudden changes in a spatial cue—would cause similar desynchronization of the ASSR as it had been observed with an interfering stimulus. The sensitivity of the 40-Hz ASSR to stimulus changes might be advantageous compared with the transient P1–N1–P2 waves of the AEF in clinical applications and neuroscience research. Therefore previously reported data (Ross et al. 2007a,b) were analyzed with respect to the ASSR. Having found that the ASSR was as sensitive as the AEF for changes in spatial location, an additional experiment has been conducted to optimize stimulus presentation rates.

METHODS

Twelve healthy young subjects (7 females, mean age 26.8 yr), 11 middle-aged (8 females, mean age 50.8 yr), and 10 older adults (5 females, mean age 71.4 yr) participated in the study. Hearing thresholds were $<$20 dB normal hearing level (HL) between 250 and 8,000 Hz for the young and middle-aged group and $<$30 dB HL $<$2,000 Hz for the older group. Interaural threshold differences were $<$10 dB for all frequencies $<$2,000 Hz for all subjects. Eighteen subjects (11 female, mean age 23.6 yr, SD 3.1 yr), who fulfilled the same criteria with respect to their hearing, participated in an additional experiment. Subjects provided their informed consent before participating in the

Address for reprint requests and other correspondence: B. Ross, Rotman Research Institute, Baycrest Centre, 3560 Bathurst Street, Toronto, ON, Canada M6A 2E1 (E-mail: bross@rotman-baycrest.on.ca).

The costs of publication of this article were defrayed in part by the payment of page charges. The article must therefore be hereby marked "*advertisement*" in accordance with 18 U.S.C. Section 1734 solely to indicate this fact.

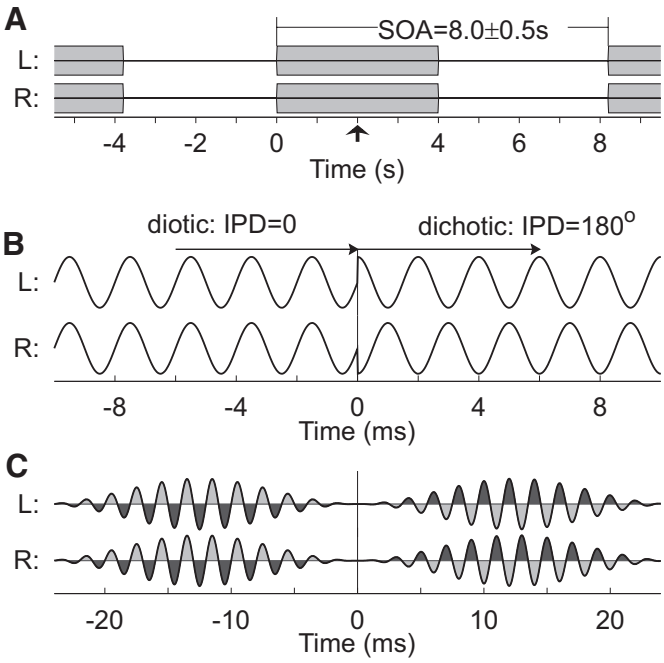

FIG. 1. Auditory stimuli. *A*: the stimulus sequence consists of tone bursts of 4.0-s duration, presented binaurally with a stimulus onset asynchrony of 7.5 to 8.5 s. The arrow at 2 s after stimulus onset indicates the time point of the change in the interaural phase difference (IPD). *B*: the 90° phase shifts of opposite directions result in a polarity reversal between left (L) and right (R) ears. Consequently, the stimulus changes from diotic sound with IPD = 0 into a dichotic sound with IPD = 180°. *C*: the phase shift occurs at the minimum of 40-Hz amplitude modulation (AM) to avoid sensation of the phase shift.

study, which was approved by the Research Ethics Board at Baycrest Centre.

Sinusoidal amplitude-modulated tones of 4.0-s duration were presented for auditory stimulation with onset asynchrony uniformly randomized between 7.5 and 8.5 s (Fig. 1*A*). At 2.0 s after stimulus onset, sudden phase shifts in the carrier signal of +90° in the left ear and −90° in the right ear, equivalent to 180° IPD change, were introduced (Fig. 1*B*). To prevent the subject from perceiving a discontinuity in the sound at the moment of the phase shift, the tones were amplitude modulated and the phase shift was set to occur at the minimum point of modulation (Fig. 1*C*). Note that the time course of the AM envelope was not affected by the carrier phase change. The stimulus carrier frequencies were 375, 500, 750, 1,000, 1,250, and 1,500 Hz, corresponding to ITDs of 1.33, 1.0, 0.66, 0.5, 0.4, and 0.33 ms, respectively, since the phase shift was always half a period. Four frequencies out of the set were presented in each group, which were 500, 1,000, 1,250, and 1,500 Hz for the young; 500, 750, 1,000, and 1,250 Hz for the middle-aged group; and 375, 500, 750, and 1,000 Hz for the older group. The frequencies were chosen according to the hypothesis that binaural performance would decrease with increasing age. The stimulus intensity was set 60 dB above individual sensation thresholds, which were measured immediately before each MEG recording. One hundred stimuli with the same carrier frequency were presented in each experimental block of 13-min duration and each block was repeated once. MEG responses to two stimulus frequencies could be recorded in a session of 1-h duration. In the first session 500 and 1,000 Hz were tested, which were the stimulus frequencies common to all age groups. The other frequencies were tested in the second session on the following day or later, with no more than 2 wk between both sessions. Stimuli were presented through Etymotic ER3A transducers connected with 1.5 m of length-matched plastic tubing and foam earplugs to the subject's ears. Plastic tubing of such length was required because the sound transducers had to be placed at a sufficient distance from the MEG sensor to avoid any interference between the stimulus signal and the recorded brain activity. Below 2,000 Hz the frequency characteristic of the sound transmission system was relatively flat (±6 dB) and the phase characteristic was linear. The phase relation between acoustical signals at both earplugs was checked using a 2-cm^3 coupler. Since insert earphones typically provide interaural attenuation of >75 dB at the frequencies used in this study, no effects of interaural cross talk were expected.

MEG recording and data analysis

MEG recordings were performed in a quiet, magnetically shielded room using a 151-channel whole-head neuromagnetometer (VSM-Medtech, Port Coquitlam, BC, Canada). The detection coils of this MEG device are almost equally spaced on the helmet-shaped surface and are configured as axial first-order gradiometers (Vrba and Robinson 2001). After low-pass filtering at 200 Hz, the magnetic field data were sampled at the rate of 625 Hz and stored continuously. MEG data were collected during passive listening, meaning that the subjects did not need to attend to the stimuli or execute a task. To control for confounding changes in vigilance, the subjects watched a closed-captioned movie of their choice, while the auditory stimuli were being presented. Compliance was verified using video monitoring. The subjects were in supine position with the head resting inside the helmet-shaped MEG sensor. The position of the MEG sensor was coregistered to the subject's head using three detection coils attached to the nasion and the left and right preauricular points. Head movements were verified to be <8 mm during each recording block. No data had to be rejected because of excessive head movements.

Each block of continuously recorded MEG data were subdivided into 100 stimulus-related epochs of 6,000-ms duration including 1,000-ms pre- and poststimulus intervals. For artifact rejection, a principal component analysis was performed on each epoch of magnetic field data. Principal components, which exceeded the threshold of 2 pT in at least one channel, were subtracted from the data. This procedure removed artifacts primarily related to dental metal and eye blinks, which are substantially larger than the brain activity. After artifact removal, the magnetic field data were averaged across epochs. To further increase the signal-to-noise ratio for the ASSR source analysis, the waveforms were averaged across all periods of the ASSR oscillation. Therefore the response waveforms in seventy 50-ms intervals from 300 to 350 ms, 325 to 375 ms, and so on to the interval from 1,950 to 2,000 ms were averaged and the same procedure was applied to the postchange stimulus data in the time interval from 2,300 to 4,000 ms. Source analysis was applied to the resulting averaged waveforms based on the model of spatiotemporal equivalent current dipoles (ECDs) in a spherical volume conductor. Single dipoles in both hemispheres were fitted simultaneously to the 151-channel magnetic field distribution. First, the data were modeled with a mirror-symmetric pair of dipoles. The resulting source coordinates were the starting points to fit the dipole in one hemisphere, whereas the coordinates in the other hemisphere were kept fixed. The last step was repeated with switching between hemispheres until the source coordinates showed no further variation. Dipole fits were accepted if the calculated field explained ≥90% of the variance of the measured magnetic field and if the SD obtained from repeated measurements was <8 mm in any Cartesian coordinate. Sixteen estimates for the dipole locations were obtained for each subject at each of the four stimulus carrier frequencies and for each of the time intervals before and after the IPD change and two repeated measurements. Locations of ASSR sources in the head-based coordinate system were compared with locations of corresponding N1 sources using paired *t*-tests. Differences were accepted as significant on the $\alpha = 0.05$ level.

The median of spatial ASSR coordinates and orientations were used as individual source models, based on which ASSR source waveforms were calculated. This procedure of source space projection (Ross et al. 2000; Tesche et al. 1995) combined the 151-channel magnetic field data into two waveforms of cortical source strength. The advantage of

analysis in source domain is that the dipole moment is independent of the sensor position. The position of the MEG sensor relative to the subject's head may change between sessions and between subjects. This may cause spatial dispersion in group-averaged magnetic field waveforms. In contrast, the waveforms of cortical source activity can be combined across repeated sessions and groups of subjects.

In an additional experiment for testing the effects of shorter interstimulus interval (ISI), the stimulus was modified so that eight IPD changes occurred in the AM sound of 4-s duration. These changes began 800 ms after stimulus onset and then recurred every 400 ms. The stimulus onset asynchrony was shortened to 5.0 s, resulting in 10-min recording time for a block of 120 stimuli. Six stimulus frequencies—500, 1,000, 1,100, 1,200, 1,300, and 1,400 Hz—were tested in a single 1-h MEG recording session. Epochs of MEG data of 800-ms length, including a 200-ms prestimulus interval, related to the time points of IPD change were averaged. Source analysis was performed on the ASSR and the P1 wave of the AEF and source waveforms of AEF and ASSR were calculated.

Three different physiological responses related to the IPD changes were obtained from the MEG data, which were stimulus-induced changes in the ASSR amplitude, the ASSR phase, and the AEF. For this data analysis, single-trial source waveforms were convolved with complex Morlet wavelets of 40-Hz center frequency and 80-ms half-intensity width (Bertrand et al. 1994). This resulted in a measure of the complex 40-Hz amplitude as a function of time. Sine and cosine of the ASSR phase at distinct time points were obtained by dividing the complex amplitude by its absolute value. Sine and cosine of single-trial phases were averaged across all trials. The inverse tangent of the mean sine and cosine terms equals the mean phase and the geometric mean (the vector length) of the mean sine and cosine terms equals the measure of phase coherence (Fisher 1993). Differences in mean phase between post- and prestimulus times were tested as an indicator for stimulus-induced changes in the ASSR phase. For all single trials the 40-Hz phase was measured at pre- and poststimulus times using the Morlet wavelet transform. A nonparametric test for differences in the distributions of pre- and poststimulus phases was based on the circular rank (Fisher 1993). ASSR amplitude differences were tested by applying a *t*-test to the difference between the squared amplitudes of pre- and poststimulus ASSRs, represented by the same wavelet coefficients as used for the ASSR phase.

AEFs were detected in individual subjects after Morlet wavelet transform of single-trial data and wavelet coefficients in the 3- to 10-Hz and 0- to 300-ms time-frequency range were tested with the Rayleigh test (Fisher 1993; for details see Ross et al. 2007b). These tests resulted in detection of a response to the IPD change in individual subjects. Whether the proportions of response detection were different for the different response measures was tested with the McNemar test (McNemar 1947). Statistical significance was accepted at $\alpha = 0.05$ for all tests.

RESULTS

ASSR sources

The group mean ASSR source locations relative to the N1 sources are given in Fig. 2. No significant differences between the age groups were found for the ASSR sources. However, ASSR sources were 8.0 mm more medially located than N1 sources in the left hemisphere [$t(34) = 7.9$, $P < 0.001$] and 7.8 mm in the right hemisphere [$t(34) = 9.6$, $P < 0.001$] and were located slightly more anterior than N1 sources [left: 2.2 mm, $t(34) = 2.1$, $P < 0.045$; right: 2.3 mm, $t(34) = 2.4$, $P < 0.02$] and more superior in both hemispheres [left: 4.0 mm, $t(34) = 3.9$, $P < 0.001$; right: 2.6 mm, $t(34) = 2.9$, $P < 0.007$]. Like N1 the ASSR sources showed a significant hemispheric asymmetry with 6.0 mm more anterior location in the right hemisphere [$t(34) = 6,8$, $P < 0.001$].

Auditory-evoked responses

Clear auditory-evoked responses were obtained for all subjects, age groups, and stimulus conditions. The example of cortical source waveforms for a young subject at 500-Hz stimulus frequency in Fig. 3 showed a P1–N1–P2 response after stimulus onset, a second one after the IPD change at 2 s, and an off-response after stimulus decay. In addition, two response types continuing for the duration of stimulus presentation became obvious, which were the sustained response, expressed as negative shift in the waveform, and the oscillating ASSR. The ASSR amplitude stayed almost constant over the entire duration of stimulus presentation with a noticeable exception of a short interval of amplitude decrement immediately after the IPD change, likely in reaction to the stimulus change.

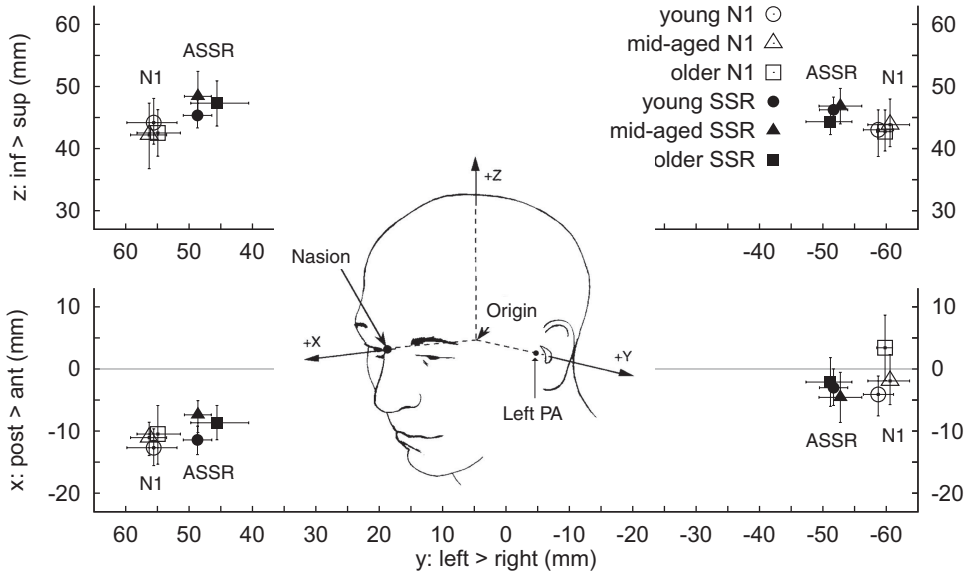

FIG. 2. Group mean locations of equivalent current dipoles for the auditory steady-state response (ASSR) and sharp negative (N1) response for the 3 age groups. The error bars denote the 95% confidence intervals for the group mean in any direction. The *inset* depicts the head-based coordinate system with the *x*-axis running from nasion to the midpoint between left and right preauricular points, the *y*-axis from right to left in the plane defined by the 3 fiducials, and the *z*-axis in inferior to superior direction. Main effects of more anterior and more medial sources of ASSR compared with N1 were common to the 3 age groups.

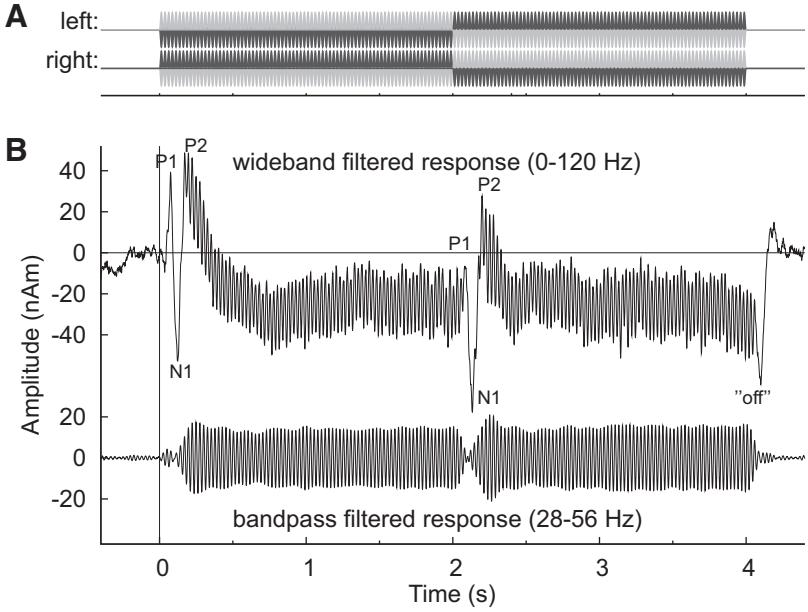

FIG. 3. Individual waveforms of auditory evoked responses (AEFs) of a young participant at 500-Hz stimulus frequency. *A*: auditory stimulus: black and gray marking of the sound wave polarities indicate the interaural phase shift at 2 s. *B*: the 0- to 120-Hz filtered response waveform (*top*) exhibits initial positive–sharp negative–slow positive (P1–N1–P2) responses of similar size at sound onset and IPD change and 2 sustained effects continuing for the stimulus duration, a negative shift, and overlaid 40-Hz oscillation. The 28- to 56-Hz band-pass filtering extracted the steady-state component (*bottom*). A clear decrement in the ASSR amplitude becomes obvious after the IPD change at 2 s.

Grand-averaged ASSR waveforms

Grand-averaged waveforms across the 12 young subjects are shown in Fig. 4 for all stimulus frequencies. The ASSR decrement following the IPD change, clearly visible at 500 Hz, however, was strongly reduced at 1,000 Hz and no longer visible at 1,250 and 1,500 Hz. If the modification of the ASSR amplitude would be a reasonable indicator of a physiological reaction to the IPD change, a threshold close to 1,500 Hz would be expected. However, the amplitude effect diminished far below 1,500 Hz. Whereas the ASSR amplitude showed dependence on IPD changes with declining effect size versus increasing stimulus frequency, the ASSR amplitude seemed not to be as sensitive for indicating the stimulus change as the N1 wave of the evoked response shown for the same data (Ross et al. 2007b).

ASSR phase deviation

Figure 5 provides a closer view of the grand-averaged ASSR waveform in the time interval around the IPD change in the young group at 500 Hz. The ASSR amplitude decreased immediately after the IPD change at 2.0, reached its minimum at latency of about 100 ms, and recovered over the following 200 ms to the steady-state value. For comparison, a sine wave representing the stimulus AM was overlaid to the ASSR waveform with the phase adjusted to the ASSR phase in the steady-state interval, thus compensating for constant time delay between stimulus and response. After the stimulus change, the ASSR began to lag behind the ongoing AM, as indicated by zero crossings of the stimulus AM signal being advanced compared with zero crossings of the ASSR. The amount of time lag increased over time, reached a maximum after about 140 ms, and decayed slowly. At about 500 ms after the stimulus change the ASSR phase had completely returned to its steady-state value. The waveforms in Fig. 5*B* also demonstrate that the total number of cycles in the ASSR equals the number of cycles in the stimulus and no cycle was missed in the response. The time course of the amount of time lag between response and stimulus (Fig. 5*C*) shows the largest time difference of 6 ms at 140 ms after the stimulus change. Given the

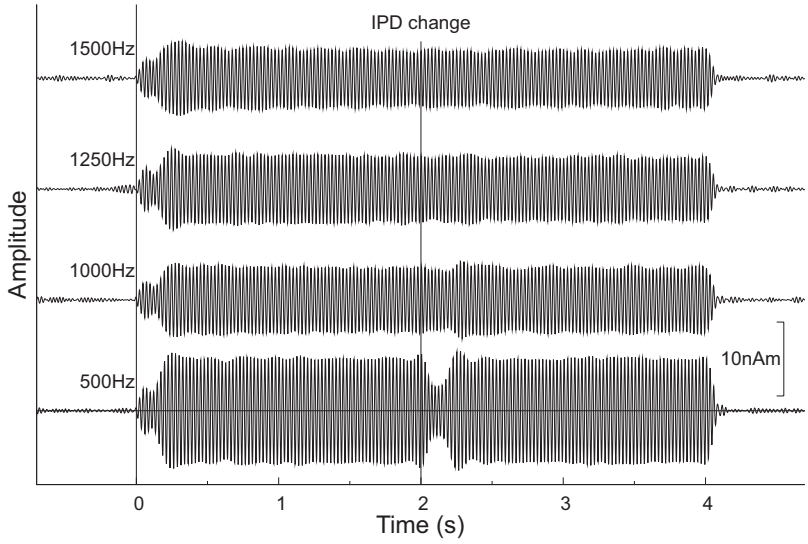

FIG. 4. Grand-averaged ASSR waveforms. The amplitude decrement after IPD change is visible in the 500-Hz response, hardly detectable at 1,000 Hz, and absent at higher frequencies.

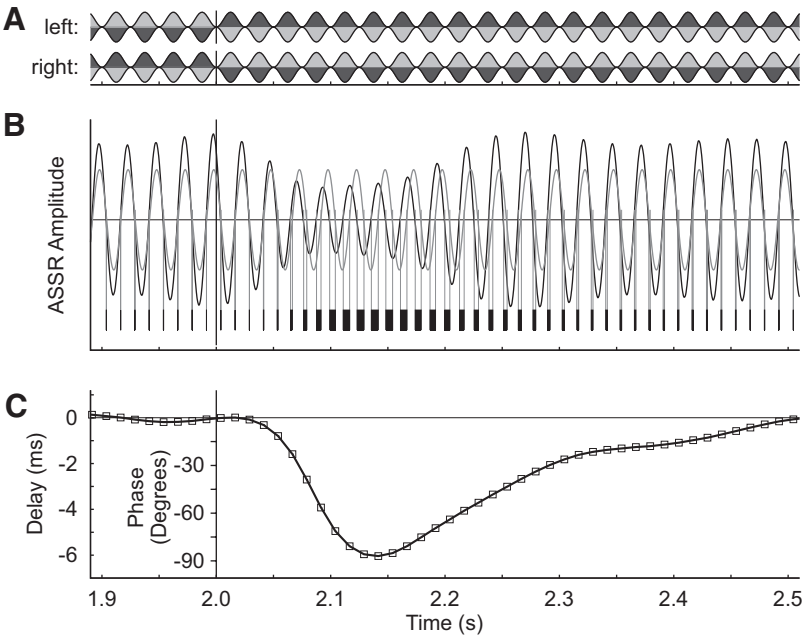

FIG. 5. ASSR phase deviation following the IPD change stimulus. *A*: auditory stimulus with carrier phase shift at $t = 2.0$ s. *B*: grand-averaged ASSR waveform to the 500-Hz stimulus in the young group (black line) in overlaid to a sinusoidal waveform representing the AM of the stimulus (gray line). Phases of stimulus AM and ASSR had been aligned for the prestimulus interval. Zero crossings of stimulus and response waveforms are indicated by vertical lines. After the IPD change stimulus the ASSR begins to lag behind the stimulus. The time differences between zero crossings of stimulus and response are indicated by black bars below the waveforms. The ASSR time lag reaches a maximum close to 150 ms after the stimulus change and decays over the time interval from 150 to 500 ms. *C*: time course of the time lag between ASSR and stimulus AM. At constant stimulation frequency of 40 Hz the time lag can be expressed as phase difference. A corresponding phase scale is drawn along the *y*-axis. The maximum time lag of 6 ms corresponds to a phase deviation of about 90°.

modulation frequency of 40 Hz, the time lag can be expressed as phase lag, and the maximum of 6 ms corresponds to about 90° or a quarter period of the 40-Hz AM.

The phase relation between ASSR and the 40-Hz modulation of the stimulus had been analyzed for the whole stimulus duration. The resulting time course of ASSR phase deviation (Fig. 6*A*) exhibited a phase lag after the stimulus onset similar to that observed after he stimulus change. The overlay of the two time courses of phase deviations after stimulus onset and stimulus change on an enlarged timescale in Fig. 6*B* showed that the return of ASSR phase after the IPD change resembled almost perfectly the ASSR phase after stimulus onset.

Possible effect of phase shift in the stimulus carrier

That the ASSR phase deviation was induced by IPD change and not by phase shift in the stimulus carrier had been demonstrated with a control condition in a single subject. A carrier phase shift of 180° was introduced in same direction for both ears in a modified 500-Hz stimulus. Thus despite the carrier phase shift the IPD did not change. AEF waveforms for both stimulus conditions (Fig. 7*A*) showed almost identical onset, sustained, and offset responses. However, the P1–N1–P2 change response was visible in case of change from diotic to dichotic stimulation only. Accordingly, the ASSR phase deviation occurred only when the stimulus phase shift constituted an IPD change but not in the case of a simultaneous phase shift in both ears (Fig. 7*B*).

Effects of stimulus frequency and age on ASSR phase deviation

Time courses of phase deviation obtained from the grand-averaged ASSR are shown for the three age groups and all stimulus frequencies in Fig. 8*A*. The graph of phase deviation at 500 Hz in the young group was already shown in Figs. 5 and 6. At a stimulus frequency of 1,000 Hz a similar time course of phase deviation had been observed, although with a smaller

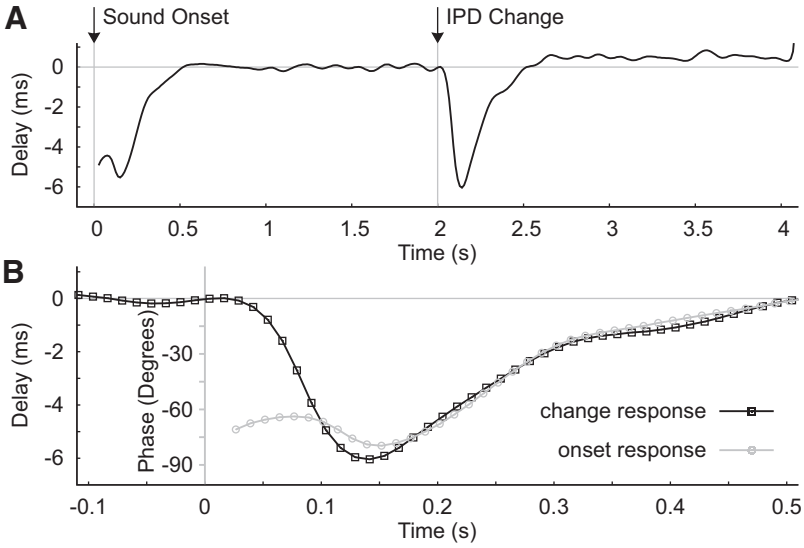

FIG. 6. Time courses of time (phase) differences between stimulus AM and the ASSR. *A*: a delay in the ASSR can be seen after stimulus onset and the IPD change. *B*: overlay of time courses of phase deviation after stimulus onset (gray line) and stimulus change (black line).

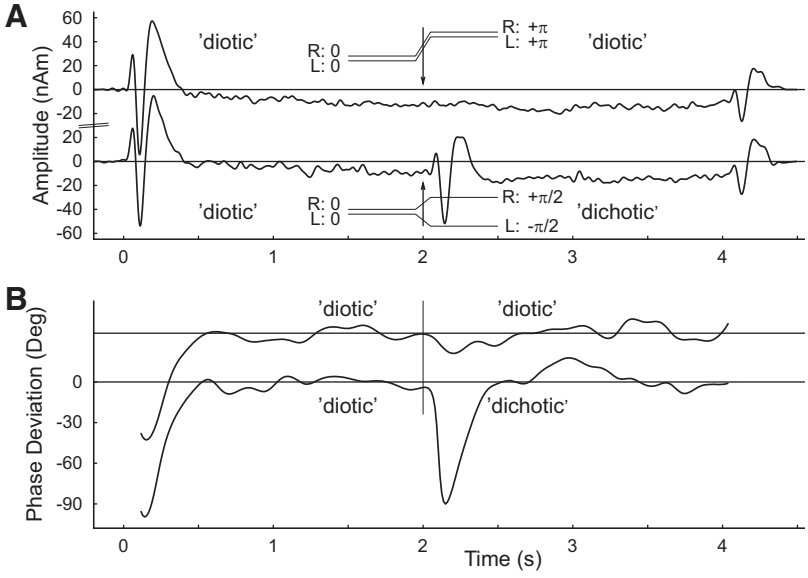

FIG. 7. A control condition with 500-Hz stimulus and phase shifts in same or opposite direction in both ears. *A*: auditory evoked responses for same phase shifts in left and right ear stimulus, which did not result in an IPD change (*top trace*) or phase shifts of opposite direction in left and right ear, which resulted in an IPD change (*bottom trace*). *B*: time courses of ASSR phase deviation in the same data show a clear effect in case of the IPD change stimulus only (*bottom trace*).

effect size. At the higher stimulus frequency of 1,250 Hz the effect of stimulus change-induced phase deviation was even less expressed and no longer visible at 1,500 Hz. Thus for the group of young subjects, a physiological threshold between 1,250 and 1,500 Hz could be accepted from visual inspection of the phase deviation time courses. In the middle-aged group the ASSR phase deviation showed a maximum of size similar to that in the young group at 500 Hz and the effect reduced progressively when the stimulus frequency increased to 750 and 1,000 Hz. Even at the highest test frequency of 1,250-Hz, small ASSR phase deviation might be visible, indicating a threshold close to 1,250 Hz. Consistently, in the group of older subjects, maximum phase deviation was on the order of 90° at the lowest stimulus frequencies of 375 and 500 Hz. The effect size decreased at higher frequencies with threshold close to 1,000 Hz. The overlay of phase time courses in Fig. 8*B* demonstrates an almost identical phase deviations for the three age groups at 500 Hz.

One observation from the time courses of phase deviation in Fig. 8*A* was that even though the effect size decreased with increasing stimulus frequency, the latency of the maximum effect was consistently around 150 ms. Thus for quantitative analysis, the amount of phase deviation at 150 ms after IPD change was measured in all individual subjects. The ANOVA

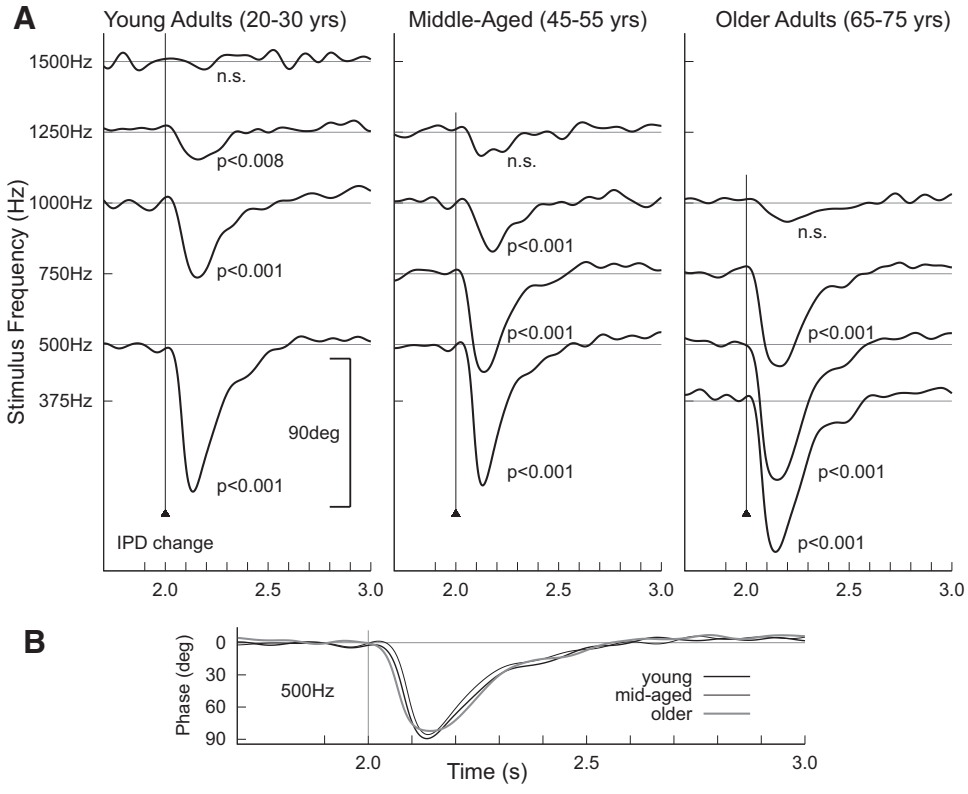

FIG. 8. *A*: time courses of ASSR phase deviation for the 3 age groups and all carrier frequencies. The *P* values below each graph resulted from a *t*-test on the group mean phase deviation at 150 ms after stimulus change. Significant ASSR phase deviations were observed ≤1,250 Hz in the young, ≤1,000 Hz in the middle-aged, and ≤750 Hz in the group of older subjects. *B*: overlay of the phase characteristics for the three age groups at 500 Hz.

with the stimulus frequency as a within-group factor (two levels, 500 and 1,000 Hz) and the age as a between-groups factor revealed a main effect of stimulus frequency [$F(1,62) = 49.5$, $P < 0.0001$], no effect of age [$F(1,62) = 2.4$], and a significant interaction between stimulus frequency and age [$F(1,62) = 15.5$, $P < 0.0003$]. With respect to the effect of frequency, a paired *t*-test showed significantly smaller phase deviation at 1,000 compared with 500 Hz in the young [$t(11) = 2.36$, $P < 0.04$], the middle-aged [$t(10) = 8.52$, $P < 0.0001$], and the older group [$t(9) = 7.28$, $P < 0.0001$]. The interaction between stimulus frequency and age resulted from different phase deviation between groups at 1,000 but not at 500 Hz. For 1,000 Hz, a *t*-test with unequal sample size revealed a significant difference between the ASSR phase deviations in the older compared with the middle-aged group [$t(19) = 2.25$, $P < 0.02$] and the older compared with the young group [$t(20) = 3.9$, $P < 0.0004$]; however, there was only a tendency to different values between young and middle-aged group [$t(21) = 1.6$, $P < 0.062$], whereas nonparametric Wilcoxon rank-sum tests showed significance for the difference between young and middle-aged ($P < 0.029$), middle-aged and older ($P < 0.026$), and young and older group ($P < 0.0008$). At 500 Hz parametric and nonparametric tests did not show significant differences between age groups.

Group mean phase deviations at 150-ms latency and corresponding 95% confidence intervals are summarized in Fig. 9, in which the characteristics of mean phase deviations were approximated by quadratic functions of the stimulus frequency for each group. The intersection of such approximation with the *x*-axis could be interpreted as threshold, indicating the stimulus frequency below which the IPD change induced a phase deviation in the ASSR. The threshold was around 1,500 Hz in the young group, 1,250 Hz in the middle-aged group, and 1,000 Hz in the older group. The significant differences at 1,000 Hz stimulus frequency and the approximated physiological thresholds indicate that the frequency range for IPD processing decreased with increasing age, and this effect commenced in midlife.

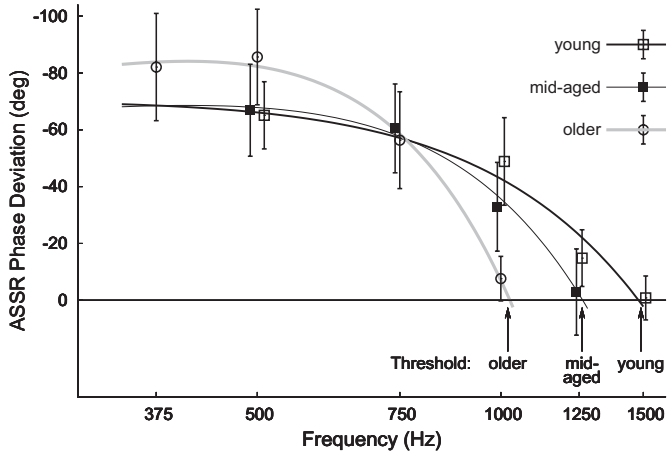

FIG. 9. Group mean ASSR phase deviation measured at 150 ms after stimulus change for all frequencies and the 3 age groups. The error bars denote the 95% confidence intervals for the group means. For each age group the characteristics of ASSR phase deviation vs. stimulus frequency was approximated by a quadratic function of frequency.

Effects of age, stimulus frequency, and hemisphere on the ASSR amplitude

ASSR amplitudes were measured and compared between stimulus conditions and age groups to investigate possible effects of aging on the ASSR-generating neural system. ANOVA was performed for the ASSR amplitudes recorded with stimulus frequencies of 500 and 1,000 Hz, which were common for all age groups. The ANOVA revealed main effects of the stimulus frequency [$F(1,126) = 40.99$, $P < 0.0001$] and hemisphere [$F(1,126) = 44.5$, $P < 0.0001$]. The subject's age had no significant effect on the ASSR amplitude [$F(2,126) = 1.64$]; however, an interaction between age and frequency was significant [$F(2,126) = 4.64$, $P < 0.012$] because the amount of ASSR amplitude decrease with increasing frequency was different in the three age groups (Fig. 10*A*). ASSR amplitude decreased between 500 and 1,000 Hz in the young group by 29.8% [$t(11) = 3.92$, $P < 0.0025$], in the middle-aged group by 24.5% [$t(11) = 4.97$, $P < 0.0005$], and in the older group by 6.5% (not significantly different from zero). ASSR amplitudes were larger in the right than in the left auditory cortex, as expressed by laterality indices, which were calculated as amplitude differences between right and left hemispheres, normalized by the sum of left and right amplitudes (Ross et al. 2005a). The right hemispheric dominance was significant for all subjects at all frequencies, except at 1,000 Hz in the middle-aged group (Fig. 10*B*).

Effects of rapid rate of IPD change

The stimulation was initially optimized for recording the P1–N1–P2 waves of the AEF with long time intervals between stimulus onset and change (2 s) and between subsequent stimulus onsets (8 s) to minimize the interactions between onset and change AEF. Because of shorter refractory time of 40-Hz ASSR, shorter intervals between subsequent IPD changes could be accepted, which resulted in a noticeable reduction of the measurement time. The effect of shortened ISI was studied in an additional experiment. Given the time course of ASSR phase deviation with maximum effect at 150 ms and about 250 ms time for recovering the steady state, ≥400-ms distance between subsequent stimulus changes was required. Thus, the stimuli for testing a rapid rate of IPD changes were 40-Hz AM tones of 4-s duration that contained eight IPD changes every 400 ms, beginning 800 ms after stimulus onset. The silent interval between the sounds was reduced to 1.0 s. Responses to six different stimulus frequencies could be recorded within a single 1-h MEG session, whereas two 1-h sessions for each subject were required for studying four frequencies in the original experiment.

Grand-averaged responses to the stimulus sequence at 500 Hz are shown in Fig. 11. Wide-band filtered responses consisted of superimposed AEF and ASSR, like the waveforms shown in Fig. 3. AEF and ASSR were separated by 24-Hz low-pass and 28- to 56-Hz band-pass filtering, respectively. The AEF waveform exhibited a P1–N1–P2 complex after stimulus onset, a negative-going sustained response continuing during the whole interval of stimulus presentation, and an offset response after stimulus decay. AEF change responses appeared overlaid to the sustained response after 800 ms and repeatedly every 400 ms. Noticeable response asymmetry de-

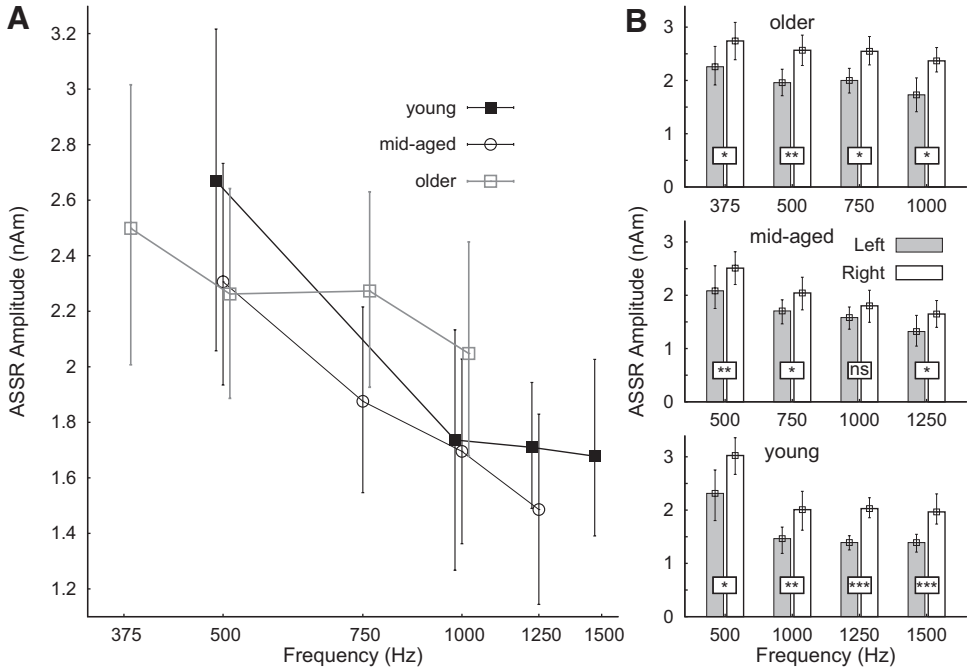

FIG. 10. Group statistics of absolute ASSR amplitudes *A*: mean ASSR amplitudes observed in left and right auditory cortices as a function of stimulus frequency for the 3 age groups. Error bars denote the 95% confidence intervals for the group mean. *B*: ASSR amplitudes in left (gray filled bars) and right (open bars) auditory cortices. The 95% confidence intervals for the group means are smaller than in the characteristics on the left because the between-subject variance has been removed. The significance levels for the hemispheric differences are indicated by asterisks (*: $\alpha = 0.05$, **: $\alpha = 0.01$, ***: $\alpha = 0.001$, n.s., not significant).

pending on the direction of IPD change became obvious from the AEF waveform in Fig. 11*B*. Responses to changes from diotic to dichotic sound showed a pronounced P1–N1–P2 complex, whereas the N1 wave was almost absent in the response to reversed IPD changes. The time series of the ASSR consisted of 40-Hz oscillations with almost constant amplitude for the duration of the stimulus. However, amplitude decrements were visible after each IPD change in the stimulus (Fig. 11*C*).

Group-averaged waveforms of responses to rapid IPD changes at all test frequencies are summarized in Fig. 12. Responses had been averaged according to stimulus changes in the same direction. Thus *time 0* in the grand-averaged responses corresponded to samples at 800, 1,600, 2,400, and 3,200 ms in the original waveform (Fig. 11). The averaged evoked responses are shown in Fig. 12*A*. The 500-Hz waveform exhibited clear P1–N1–P2 waves for the first response, elicited by a stimulus transition from diotic to dichotic sound. The second response after the reversed stimulus change from dichotic to diotic sound at 400 ms showed a P1 wave of similar amplitude as the first response, albeit a strongly reduced N1 response. Thus the second AEF resembled a single positive wave as the combined effect of P1 and P2 waves. The strongest difference in configuration of the AEF shown for long ISI in Figs. 3 and 7 and for rapid changes in Fig. 12*A* was the largely reduced N1 amplitude. However, a clear P1–N1–P2 wave could be observed ≤1,200 Hz for the stimulus change from diotic to dichotic sound.

Time courses of ASSR phase at 500 Hz (Fig. 12*B*) showed the strongest deviation of about 50° at 150 ms after the stimulus change from diotic to dichotic sound and 32° for change in the reversed direction. This response asymmetry was

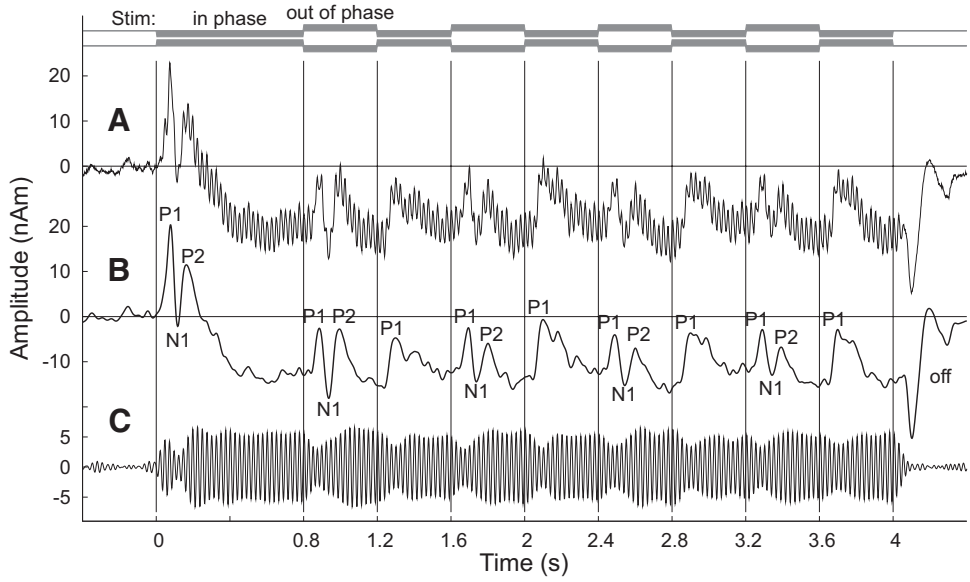

FIG. 11. Grand-averaged waveforms (n = 18 subjects, left and right auditory cortices) of evoked responses to rapid changes in the IPD at 500-Hz stimulus frequency. The horizontal bars at the *top* depict the sequence of IPD changes in the stimulus. For the first 800 ms left and right ear sounds are in phase. At 800 ms the IPD changes from 0 to 180° and the left and right ear sounds are out of phase for 400 ms. IPD phase changes occur every 400 ms until the end of the 4-s stimulus. *A*: wide band (0–120 Hz) filtered response. *B*: the 24-Hz low-pass filtered response shows a P1–N1–P2 complex after the stimulus onset and for the stimulus transitions from "in-phase" to "out-of-phase" sound. The responses to IPD changes in reverse direction show a P1 wave, although a strongly reduced N1 wave only. *C*: bandpass filtering at 28 to 56 Hz extracted the ASSR waveform. The ASSR time series exhibits amplitude decrements after all stimulus changes.

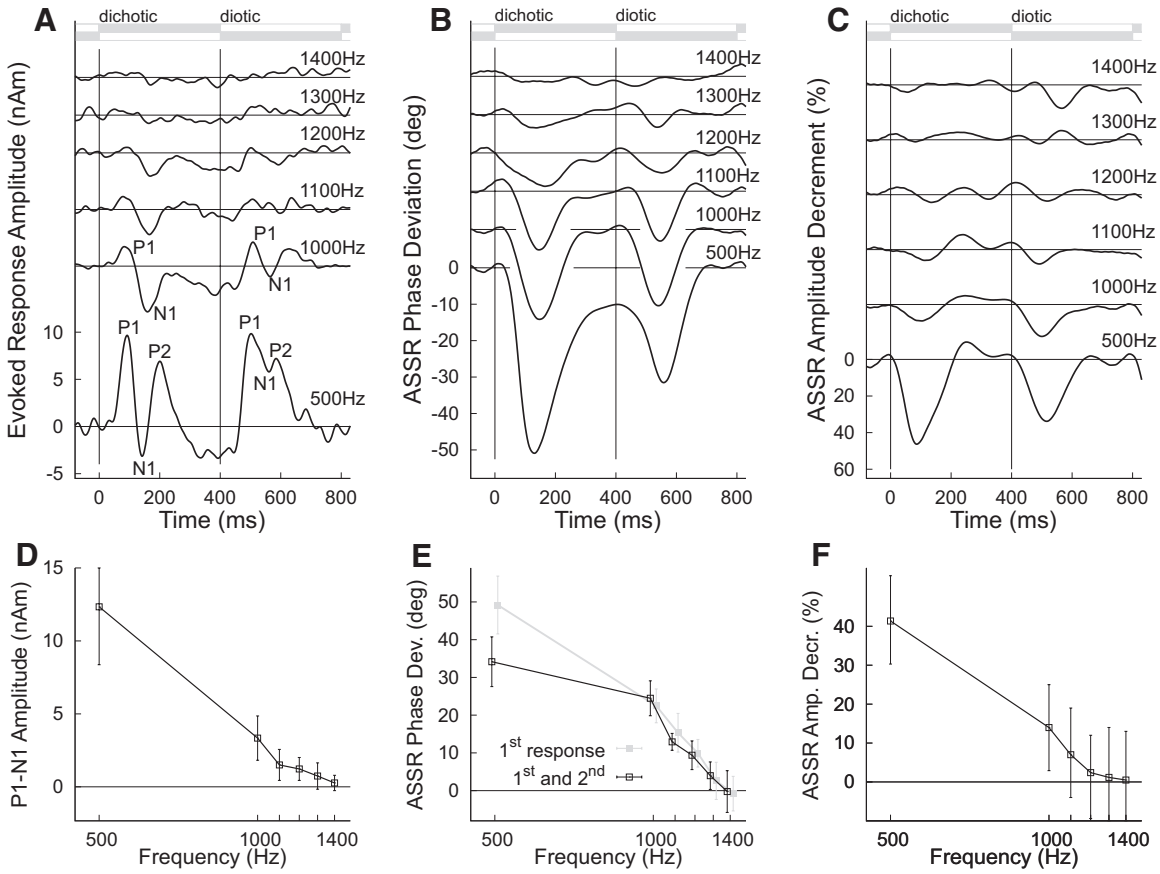

FIG. 12. Time courses of ASSR change and corresponding AEF at 6 stimulus frequencies. Time zero corresponds to the stimulus change from same sound at both ears (0° IPD, diotic sound) to sounds of opposite phase (180° IPD, dichotic sound) and 0.4 s corresponds to the stimulus change in reverse order. *A*: averaged waveform of stimulus change evoked responses. *B*: time courses of ASSR phase deviation averaged across all subjects ($n = 18$) and all occurrences of IPD change. *C*: time courses of stimulus change induced amplitude decrement in the ASSR. For all 3 measures asymmetric responses with respect to the direction of stimulus change are obvious. *D*: characteristics of the group mean AEF amplitude, measured between P1 and N1 peak for the response to the change from diotic to dichotic stimulus, as a function of the stimulus frequency. The error bars denote the 95% confidence intervals for the group mean. *E*: characteristics of the group mean of ASSR phase deviation at latency of 150 ms after the stimulus change as function of the stimulus frequency. Shown are the characteristics for stimulus changes in both directions. *F*: corresponding characteristics of the amount of ASSR amplitude decrement at 100-ms latency.

significant across the group [$t(17) = 6.8$, $P < 0.001$]. The amount of phase deviation and the response asymmetry decreased with increasing frequency. Amplitude changes (Fig. 12*C*) were strongest at 500 Hz with 45% amplitude decrement for the first response and 35% to stimulus change in the reversed direction. Mean latencies were around 100 ms, i.e., earlier than the maximum phase deviation at 150 ms. The amplitude effect was reduced to about one third of the size at 500 Hz at 1,000 Hz and no longer different from baseline fluctuations at ≥1,200 Hz.

Characteristics of the group mean values of ASSR phase deviation, ASSR amplitude decrement, and the AEF amplitude as a function of the stimulus frequency are shown in Fig. 12, *D–F*. The measure of AEF amplitude was significant for frequencies ≤1,200 Hz, the ASSR phase ≤1,200 or 1,300 Hz, and the ASSR amplitude ≤1,000 Hz. Although all three characteristics established a threshold in the 1,000- to 1,300-Hz range, the ASSR phase showed the steepest slope toward the threshold. Likely, the threshold could be more robustly determined when using the ASSR phase than an AEF amplitude measure.

Proportions of individuals in whom a change response could be detected indicated the performance in threshold detection using different response measures. At the lowest stimulus frequency of 500 Hz, AEF and ASSR phase deviations were detected in all subjects, whereas ASSR amplitude was significant in only 10 of 18 subjects. The McNemar test revealed superior response detection using ASSR phase compared with amplitude ($P < 0.004$). At 1,000-Hz stimulus frequency ASSR phase deviations were found in 14 individuals compared with ASSR amplitude changes in 6 ($P < 0.012$) and AEF in 8 subjects ($P < 0.016$). At 1,100 Hz individual response detection was significant in 7, 1, and 5 subjects for the ASSR phase, ASSR amplitude, and the AEF, respectively. In two subjects the ASSR phase deviation was significant at 1,200 Hz, but in none at 1,300 and 1,400 Hz. Response detection based on the AEF or ASSR amplitude was not significant in any subject at frequencies of 1,200 to 1,400 Hz.

DISCUSSION

The main result of the study was that IPD changes in 40-Hz AM sound induced desynchronization of ongoing ASSR, which was expressed as a decrease in amplitude and delayed phase. Time courses of ASSR phase deviation established a new type of auditory change response. The ASSR change

response robustly reproduced previous results of the effects of stimulus frequency and age on the AEF in response to IPD changes, although slightly higher threshold frequencies were found here. ASSR change responses could be recorded at a rapid stimulus presentation rate and showed a response asymmetry with the greatest effect when the stimulus changed from diotic to dichotic sound. Furthermore, measuring 40-Hz ASSR in subjects over a wide age range gave insights into the possible effects of aging on the ASSR. The discussion focuses on the nature of the observed responses and its application in studying the effect of aging on IPD detection.

Origin of the 40-Hz ASSR

Despite small amplitudes, ASSRs could be reliably recorded with MEG. Underlying sources were modeled with single equivalent current dipoles in left and right hemispheres and were compared with the sources of simultaneously recorded N1 responses. The finding of more medial and more anterior located ASSR sources compared with N1 is consistent with an earlier MEG study (Herdman et al. 2003). The N1 response results from multiple sources with the strongest contribution from lateral parts of Heschl's gyrus and the planum temporale, as previously shown from intracranial and MEG recordings in the same patients (Godey et al. 2001). Single equivalent sources in MEG represent the center of gravity of such source configuration and had been localized in several studies in the planum temporale (Lutkenhoner and Steinstrater 1998; Pantev et al. 1995). This region, posterior and adjacent to Heschl's gyrus, has been identified as nonprimary auditory cortex in histological studies (Galaburda and Sanides 1980; Rivier and Clarke 1997). The spatial relation between N1 and ASSR sources gives evidence for ASSR originating from medial parts of Heschl's gyrus, which has been identified as primary auditory cortex (Rademacher et al. 2001). The finding of ASSR sources in primary auditory cortical areas corroborates results of earlier MEG studies in human (Gutschalk et al. 1999; Hari et al. 1989; Makela and Hari 1987) and intracortical and subdural recordings in animals (Eggermont 1997; Franowicz and Barth 1995). Besides main sources of ASSR in primary auditory cortices likely a wider network of cortical and subcortical generators is involved (Herdman et al. 2002).

Functional meaning of 40-Hz ASSR

Gamma-band activity in the 40-Hz range has been addressed to perception and cognition (Kaiser and Lutzenberger 2003). For auditory perception, Herrmann et al. (2004) proposed that early gamma oscillations (before 100 ms) relate to matching the incoming auditory information after sensory encoding and feature integration with the actual contents of a sensory memory and that late gamma activity (between 200 and 300 ms) reflects utilization of the stored memory as well as wide-range communication to coordinate behavioral performance related to the stimulus. Early gamma activity has been observed in specific sensory areas as stimulus locked burst of oscillation (Gruber et al. 2006; Pantev et al. 1991). Tallon-Baudry and Bertrand (1999) described the later gamma oscillations as not phase locked to the stimulus onset and supported the functional meaning of object representation and maintaining of sensory information. Such a type of gamma-band activity is difficult to record and to separate from background electroencephalogram (EEG) or MEG. The steady-state method overcomes this problem by driving the underlying neural network into a highly synchronized state. Corresponding steady-state responses are phase-locked to the stimulus rhythm and can be separated from noise by signal averaging in time or frequency domain. This approach is consistent with the interpretation of previous findings that the ASSR relates to robust representation of the auditory stimulus (Ross and Pantev 2004; Ross et al. 2005b). Initially, it was thought that the ASSRs are repeatedly superimposed early evoked gamma activity or the middle latency responses (Galambos et al. 1981). However, several experimental observations were not compatible with this explanation (Ross et al. 2002; Santarelli and Conti 1999) and, likely, the ASSR relates to stimulus synchronized late gamma-band activity.

Specificity of the response to IPD changes

A novel finding was that the IPD change in the stimulus induced a change in the time course of the ASSR and established a new type of auditory-evoked change response. From the observation of decreasing and vanishing ASSR change response with higher stimulus frequency, which parallels behavioral performance in IPD detection, it can be concluded that the ASSR deviation was induced by a perceivable change in the IPD. The stimulus frequency characteristics of the ASSR change response closely matched the previously observed characteristic for the effect on the AEF. Moreover, the effect of aging observed with the AEF could be reproduced with the ASSR change. The alternative explanation—that the ASSR change has been elicited by the physical phase change in the stimulus and this confound could depend in same way on stimulus frequency as the IPD—seems unlikely because the phase change could not be perceived from each monaural sound (Ross et al. 2007b). Moreover, results of a control condition demonstrated that phase shifts in the stimulus without changing the IPD did not induce an ASSR change response nor did it elicit an AEF.

ASSR change is most reliably expressed as a phase change

The stimulus change induced a change in amplitude and phase of the ASSR. However, the ASSR phase deviation was a more robust measure than the amplitude change. When the overall response decreased with increasing frequency, group mean ASSR phase changes, but no amplitude changes, were visible at higher frequencies. Furthermore, the proportion of response detection in individuals was significantly higher for phase changes than for the amplitude effect. Although the steady state is defined by constant amplitude and phase, phase synchronization characterizes the 40-Hz ASSR better than constant amplitude. Amplitude fluctuations in the ASSR have not been systematically investigated, mainly because the ASSR is commonly analyzed in the frequency domain and the amplitude is integrated over time. Indirect evidence for better characterization of ASSR by its phase properties came from comparisons of data analysis methods, which have often found phase statistics superior over amplitude statistics (Dobie and Wilson 1994; Picton et al. 2001).

Moreover, the ASSR phase deviation always occurred in the same direction; the stimulus induced a phase lag of ASSR

behind the stimulus and a characteristic time course of return into the steady state. In particular, the time course of phase return closely resembled the time course of ASSR phase during the ASSR onset (Ross et al. 2002), after changes in the periodicity of the stimulus (Ross and Pantev 2004), and induced by an interfering stimulus (Ross et al. 2005b). The observed time course of ASSR change in the current study is consistent with previous studies. These findings suggest that synchronized oscillations dynamically establish a network for representing current auditory objects. An occasional change in the auditory environment requires updating the internal representation. Thus the existing network configuration has to be dissolved and a new one has to be established. The reset of 40-Hz oscillations may reflect such a dynamic reconfiguration. The amount of phase changes less than $\pi/2$ was consistent across all studies. A phase transient of $\pi/2$ is characteristic for the time interval of synchronization of a harmonic oscillator with a loosely coupled driving oscillating force (Rosenblum and Pikovsky 2003) and supports the hypothesis of a stimulus-induced dynamic network reconfiguration.

ASSR change response

Naatanen and Picton (1987) distinguished two types of auditory change response depending on whether the stimulus changed in level (e.g., a change in loudness from silence to audible sound) or changed in a characteristic feature within ongoing sound (e.g., changing frequency). They proposed that the latter type requires some form of memory and a neural mechanism to compare it with the current sound input. Because the stimulus energy did not change, the ASSR change response reported in this study belongs to the second type of change responses. The involvement of memory is especially compatible with the concept that the ASSR reflects an internal stimulus representation.

The alternative explanation that the change response was actually an onset response to the new version of the stimulus would be reasonable if the information carried in the acoustical signal before and after the change was processed in separated channels, respectively. Given, for example, the tonotopic organization along the auditory pathway, the response to a sudden frequency step of reasonable size could be explained with switching between frequency channels and the response could be explained as the onset response produced by newly involved resources. The similarity between onset and change responses and between time courses of ASSR deviation after stimulus onset or change would indeed support such a hypothesis.

However, the concept of information channels has been exploited in much deeper detail. A sound object is not defined by just one feature, such as the sound frequency, but consists of multiple properties such as loudness, sound location, timbre, and even more complex information in music and speech sound. A currently discussed concept proposes parallel processing of different sound features in separate pathways, which are differently defined from the physical auditory channels. A prominent example for parallel auditory pathways is the "what and where" dissociation, which was originally established in the visual system (Rauschecker and Tian 2000).

Sound processing in the current study could be discussed in terms of two pathways. One contained the AM sound, defined by its carrier and modulation frequencies, modulation depth, intensity, and duration, and was perceived as ongoing sound with certain pitch, roughness, and loudness. The other carried location information with two types of percepts, the sound centered in the head or a spacious sound heard with both ears. The rhythm of 40-Hz modulation, carried in one pathway only, evoked the ASSR. The change in location information carried in the second pathway induced the change response. That means a change in the stimulus context, here the spatial information, interfered with the otherwise continuous stimulus and caused the change response. This interpretation extends our previous findings that a concurrent stimulus (Ross et al. 2005b) or change in stimulus rhythm (Ross and Pantev 2004) desynchronized the ASSR to a more general concept. This result opens a new field of possible experiments in which the sensory environment would be modified in parallel to ongoing steady-state stimulation and effects of stimulus changes on the steady-state responses would be observed. Future work should address the question whether stimuli in other sensory modalities would interact with the 40-Hz ASSR.

Effects of aging on the ASSR amplitude

The finding that 40-Hz ASSR amplitudes were not significantly affected by aging is consistent with previous reports. However, subject variability is commonly large in such studies and amplitude effects may not reach significance, given the typically small sample size (Picton et al. 2003). Despite changes in amplitude and latency of N1 responses, Muchnik et al. (1993) found no differences in the ASSR between young (18–40 yr) and older (60–77 yr) adults for 500-Hz tone-pip stimuli. An increase in ASSR amplitude during childhood and adolescence had been found in an MEG study with 40-Hz click train stimulation, although amplitudes were constant in adulthood between 25 and 52 yr (Rojas et al. 2006). A tendency for increased ASSR had been reported by Poulsen et al. (2007) for adults (19–45 yr) in an EEG study with 40-Hz frequency modulated stimuli. Purcell et al. (2004) reported a tendency for lower ASSR amplitudes in the elderly and suggested that the effect of aging may be more expressed as a shift in the ASSR peak frequency, which was 41 Hz in young and 37 Hz in older adults. Given this shift in best frequency of the ASSR, the choice of 40 Hz in the current study was more optimal for the young than for the older group and smaller responses in the older group could have been observed for this reason. However, this was not the case and it seems that 40-Hz ASSR does not deteriorate with aging.

Consistent with the current results Leigh-Paffenroth and Fowler (2006) found no main effect of age on the 40-Hz ASSR amplitude but an interaction between stimulus frequency and age expressed as better detectable responses at 500 Hz compared with 4,000 Hz in the young but not in the older group. This observation is consistent with the present finding that the negative slope in the characteristics of ASSR amplitude versus stimulus carrier frequency was less expressed in the older than in the younger group. Decreasing ASSR amplitude with increasing carrier frequency, as reported consistently (Galambos et al. 1981; Picton et al. 1987; Rodriguez et al. 1986; Ross et al. 2000), had been attributed to a larger activation pattern in the cochlea at lower frequencies (Picton et al. 2003). Thus aging-related changes in the ASSR frequency characteristic are likely

related to changes in the auditory periphery with advancing age.

Characteristic features of the 40-Hz ASSR, such as the right hemispheric dominance and the time constants of the ASSR change, were remarkably reproduced between age groups. This could be interpreted as further evidence against an aging-related decline in the 40-Hz ASSR-generating neural networks. It had been assumed that the ASSR reflects auditory temporal acuity (Purcell et al. 2004) and it seems that the neural encoding of auditory events on a timescale of tens of milliseconds is not affected by aging.

Effects of aging on IPD detection

Our previously reported results about P1–N1–P2 responses in the same data (Ross et al. 2007a)—showing a physiological threshold for the detection of IPD changes and that this threshold decreased with increasing age—were reproduced based on the ASSR change response. Significant differences in the ASSR phase deviation between the young and middle-aged and between the middle-aged and older groups corroborated the finding that binaural hearing based on IPD is already affected in midlife. The results indicate an aging-related limitation of the frequency range for phase-locked processing at the level of the auditory brain stem. Overall, slightly higher frequency limits were found for the same data, which likely indicates higher sensitivity of the ASSR phase change compared with the AEF. The interpretation of the presently observed age effect is completely in line with the previously reported results based on AEF.

ASSR at rapid stimulus change

The ASSR change response could be successfully demonstrated at a higher stimulation rate of 2.5 IPD changes per second. Detecting the physiological threshold for IPD changes had been shown in a group of young subjects. The reduction of recording time by a factor of 2 and increasing the number of test frequencies from four to six demonstrated the practical usability of the new approach. Response detection using ASSR change responses was superior to response detection based on AEF. However, a fair comparison between AEF and ASSR change response should be based on optimal stimulus timing for each approach, respectively. Such systematic work—studying the characteristic relation between ASSR change response size and rate of stimulus changes—must still be done. Nevertheless, for investigating fast stimulus changes, the ASSR change response could be the right method of choice.

Response asymmetry

Change responses were larger for IPD transition from 0 to 180° than for the reverse direction. This is consistent with a previous finding of 10% larger N1 amplitude for changes from diotic to dichotic sound than for the reverse direction and 10% larger onset N1 for dichotic sound than for the diotic sound (Ross et al. 2004). Response asymmetry of same size was previously reported for changes in interaural correlation of a noise stimulus, which induces a similar percept as in the current study, in EEG (Jones et al. 1991) and MEG (Chait et al. 2005). Chait et al. (2007a,b) provided an interpretation for the response asymmetry as modification of cortical responses by the particular auditory context. Another interpretation would be that two sounds perceived with dichotic stimulation provided a stronger input than one sound perceived in the diotic condition. Importantly, the finding of stimulus asymmetry supports the interpretation that the ASSR change response was specific to the IPD change.

Conclusions

The stimulus-induced temporal dynamics of auditory 40-Hz steady-state responses represents a novel type of auditory response. Practical application has been successfully demonstrated on a study of the effect of aging on processing of interaural phase differences.

ACKNOWLEDGMENTS

I thank Dr. Terence Picton for comments on an earlier version of the manuscript.

GRANTS

This work was supported by Canadian Institutes of Health Research Grant MOP-81135, the Canadian Foundation for Innovation, and The Hearing Foundation of Canada.

REFERENCES

Bertrand O, Bohorquez J, Pernier J. Time-frequency digital filtering based on an invertible wavelet transform: an application to evoked potentials. *IEEE Trans Biomed Eng* 41: 77–88, 1994.

Chait M, Poeppel D, de Cheveigné A, Simon JZ. Human auditory cortical processing of changes in interaural correlation. *J Neurosci* 25: 8518–8527, 2005.

Chait M, Poeppel D, de Cheveigné A, Simon JZ. Processing asymmetry of transitions between order and disorder in human auditory cortex. *J Neurosci* 27: 5207–5214, 2007a.

Chait M, Poeppel D, Simon JZ. Stimulus context affects auditory cortical responses to changes in interaural correlation. *J Neurophysiol* 98: 224–231, 2007b.

Culling JF, Hawley ML, Litovsky RY. The role of head-induced interaural time and level differences in the speech reception threshold for multiple interfering sound sources. *J Acoust Soc Am* 116: 1057–1065, 2004.

Dobie RA, Wilson MJ. Objective detection of 40 Hz auditory evoked potentials: phase coherence vs. magnitude-squared coherence. *Electroencephalogr Clin Neurophysiol* 92: 405–413, 1994.

Eggermont JJ. Firing rate and firing synchrony distinguish dynamic from steady state sound. *Neuroreport* 8: 2709–2713, 1997.

Fisher NI. *Statistical Analysis of Circular Data.* Cambridge, UK: Cambridge Univ. Press, 1993.

Franowicz MN, Barth DS. Comparison of evoked potentials and high-frequency (gamma-band) oscillating potentials in rat auditory cortex. *J Neurophysiol* 74: 96–112, 1995.

Galaburda A, Sanides F. Cytoarchitectonic organization of the human auditory cortex. *J Comp Neurol* 190: 597–610, 1980.

Galambos R, Makeig S, Talmachoff PJ. A 40-Hz auditory potential recorded from the human scalp. *Proc Natl Acad Sci USA* 78: 2643–2647, 1981.

Godey B, Schwartz D, de Graaf JB, Chauvel P, Liegeois-Chauvel C. Neuromagnetic source localization of auditory evoked fields and intracerebral evoked potentials: a comparison of data in the same patients. *Clin Neurophysiol* 112: 1850–1859, 2001.

Gruber T, Trujillo-Barreto NJ, Giabbiconi CM, Valdes-Sosa PA, Muller MM. Brain electrical tomography (BET) analysis of induced gamma band responses during a simple object recognition task. *Neuroimage* 29: 888–900, 2006.

Gutschalk A, Mase R, Roth R, Ille N, Rupp A, Hahnel S, Picton TW, Scherg M. Deconvolution of 40 Hz steady-state fields reveals two overlapping source activities of the human auditory cortex. *Clin Neurophysiol* 110: 856–868, 1999.

Hari R, Hamalainen M, Joutsiniemi SL. Neuromagnetic steady-state responses to auditory stimuli. *J Acoust Soc Am* 86: 1033–1039, 1989.

Hawley ML, Litovsky RY, Culling JF. The benefit of binaural hearing in a cocktail party: effect of location and type of interferer. *J Acoust Soc Am* 115: 833–843, 2004.

Herdman AT, Lins O, Van Roon P, Stapells DR, Scherg M, Picton TW. Intracerebral sources of human auditory steady-state responses. *Brain Topogr* 15: 69–86, 2002.

Herdman AT, Wollbrink A, Chau W, Ishii R, Ross B, Pantev C. Determination of activation areas in the human auditory cortex by means of synthetic aperture magnetometry. *Neuroimage* 20: 995–1005, 2003.

Herrmann CS, Munk MH, Engel AK. Cognitive functions of gamma-band activity: memory match and utilization. *Trends Cogn Sci* 8: 347–355, 2004.

Jones SJ, Pitman JR, Halliday AM. Scalp potentials following sudden coherence and discoherence of binaural noise and change in the inter-aural time difference: a specific binaural evoked potential or a "mismatch" response? *Electroencephalogr Clin Neurophysiol* 80: 146–154, 1991.

Kaiser J, Lutzenberger W. Induced gamma-band activity and human brain function. *Neuroscientist* 9: 475–484, 2003.

Leigh-Paffenroth ED, Fowler CG. Amplitude-modulated auditory steady-state responses in younger and older listeners. *J Am Acad Audiol* 17: 582–597, 2006.

Lutkenhoner B, Steinstrater O. High-precision neuromagnetic study of the functional organization of the human auditory cortex. *Audiol Neurootol* 3: 191–213, 1998.

Makela JP, Hari R. Evidence for cortical origin of the 40 Hz auditory evoked response in man. *Electroencephalogr Clin Neurophysiol* 66: 539–546, 1987.

McNemar Q. Note on the sampling error of the difference between correlated proportions or percentages. *Psychometrika* 12: 153–157, 1947.

Muchnik C, Katz-Putter H, Rubinstein M, Hildesheimer M. Normative data for 40-Hz event-related potentials to 500-Hz tonal stimuli in young and elderly subjects. *Audiology* 32: 27–35, 1993.

Naatanen R, Picton T. The N1 wave of the human electric and magnetic response to sound: a review and an analysis of the component structure. *Psychophysiology* 24: 375–425, 1987.

Pantev C, Bertrand O, Eulitz C, Verkindt C, Hampson S, Schuierer G, Elbert T. Specific tonotopic organizations of different areas of the human auditory cortex revealed by simultaneous magnetic and electric recordings. *Electroencephalogr Clin Neurophysiol* 94: 26–40, 1995.

Pantev C, Makeig S, Hoke M, Galambos R, Hampson S, Gallen C. Human auditory evoked gamma-band magnetic fields. *Proc Natl Acad Sci USA* 88: 8996–9000, 1991.

Picton TW, Dimitrijevic A, John MS, Van Roon P. The use of phase in the detection of auditory steady-state responses. *Clin Neurophysiol* 112: 1698–1711, 2001.

Picton TW, John MS, Dimitrijevic A, Purcell D. Human auditory steady-state responses. *Int J Audiol* 42: 177–219, 2003.

Picton TW, Skinner CR, Champagne SC, Kellett AJ, Maiste AC. Potentials evoked by the sinusoidal modulation of the amplitude or frequency of a tone. *J Acoust Soc Am* 82: 165–178, 1987.

Poulsen C, Picton TW, Paus T. Age-related changes in transient and oscillatory brain responses to auditory stimulation in healthy adults 19–45 years old. *Cereb Cortex* 17: 1454–1467, 2007.

Purcell DW, John SM, Schneider BA, Picton TW. Human temporal auditory acuity as assessed by envelope following responses. *J Acoust Soc Am* 116: 3581–3593, 2004.

Rademacher J, Morosan P, Schormann T, Schleicher A, Werner C, Freund HJ, Zilles K. Probabilistic mapping and volume measurement of human primary auditory cortex. *Neuroimage* 13: 669–683, 2001.

Rauschecker JP, Tian B. Mechanisms and streams for processing of "what" and "where" in auditory cortex. *Proc Natl Acad Sci USA* 97: 11800–11806, 2000.

Rees A, Green GG, Kay RH. Steady-state evoked responses to sinusoidally amplitude-modulated sounds recorded in man. *Hear Res* 23: 123–133, 1986.

Rivier F, Clarke S. Cytochrome oxidase, acetylcholinesterase, and NADPH-diaphorase staining in human supratemporal and insular cortex: evidence for multiple auditory areas. *Neuroimage* 6: 288–304, 1997.

Rodriguez R, Picton TW, Linden D, Hamel G, Laframboise G. Human auditory steady state responses: effects of intensity and frequency. *Ear Hear* 7: 300–313, 1986.

Rojas DC, Maharajh K, Teale PD, Kleman MR, Benkers TL, Carlson JP, Reite ML. Development of the 40-Hz steady state auditory evoked magnetic field from ages 5 to 52. *Clin Neurophysiol* 117: 110–117, 2006.

Rosenblum M, Pikovsky A. Synchronization: from pendulum clocks to chaotic lasers and chemical oscillators. *Contemp Physics* 44: 401–416, 2003.

Ross B, Borgmann C, Draganova R, Roberts LE, Pantev C. A high-precision magnetoencephalographic study of human auditory steady-state responses to amplitude-modulated tones. *J Acoust Soc Am* 108: 679–691, 2000.

Ross B, Fujioka T, Tremblay KL, Picton TW. Aging in binaural hearing begins in mid-life: evidence from cortical auditory-evoked responses to changes in interaural phase. *J Neurosci* 27: 11172–11178, 2007a.

Ross B, Herdman AT, Pantev C. Right hemispheric laterality of human 40 Hz auditory steady-state responses. *Cereb Cortex* 15: 2029–2039, 2005a.

Ross B, Herdman AT, Pantev C. Stimulus induced desynchronization of human auditory 40-Hz steady-state responses. *J Neurophysiol* 94: 4082–4093, 2005b.

Ross B, Herdman AT, Wollbrink A, Pantev C. Auditory cortex responses to the transition from monophonic to pseudo-stereo sound. *Neurol Clin Neurophysiol* 2004: 18(1–4), 2004.

Ross B, Pantev C. Auditory steady-state responses reveal amplitude modulation gap detection thresholds. *J Acoust Soc Am* 115: 2193–2206, 2004.

Ross B, Picton TW, Pantev C. Temporal integration in the human auditory cortex as represented by the development of the steady-state magnetic field. *Hear Res* 165: 68–84, 2002.

Ross B, Tremblay KL, Picton TW. Physiological detection of interaural phase differences. *J Acoust Soc Am* 121: 1017–1027, 2007b.

Santarelli R, Conti G. Generation of auditory steady-state responses: linearity assessment. *Scand Audiol Suppl* 51: 23–32, 1999.

Stevens SS. The localization of actual sources of sound. *Am J Psychol* 48: 297–306, 1936.

Tallon-Baudry C, Bertrand O. Oscillatory gamma activity in humans and its role in object representation. *Trends Cogn Sci* 3: 151–162, 1999.

Tesche CD, Uusitalo MA, Ilmoniemi RJ, Huotilainen M, Kajola M, Salonen O. Signal-space projections of MEG data characterize both distributed and well-localized neuronal sources. *Electroencephalogr Clin Neurophysiol* 95: 189–200, 1995.

Vrba J, Robinson SE. Signal processing in magnetoencephalography. *Methods* 25: 249–271, 2001.